Density functional approach on wetting behavior of binary associating mixtures

Ming-Chih Yeh and Li-Jen Chen[a)]
Department of Chemical Engineering, National Taiwan University, Taipei, Taiwan 106, Republic of China

(Received 24 December 2002; accepted 11 February 2003)

A density functional theory is applied to study wetting behaviors of binary associating mixtures, which are described by the statistical associating fluid theory of Wertheim. When the associating interaction is strong, the phase behavior of the binary associating mixture falls into the type-VI mixtures of the classification scheme of van Konynenburg and Scott. There are two types of closed-loop phase behaviors for the type-VI mixture. That is, a closed-loop phase diagram for vapor–liquid–liquid coexistence (along its triple line) at low pressures and the other one for liquid–liquid coexistence at a relatively high pressure. In this study, the wetting behavior of the lower liquid phase at the surface of the upper liquid phase is carefully examined for both vapor–liquid–liquid coexistence and liquid–liquid coexistence regimes. In the latter regime, a third inert air phase is introduced since wetting behavior always involves three phases. For both regimes the binary associating mixture exhibits a sequence of wetting transitions, complete wetting→partial wetting →complete wetting, along with increasing temperature. The order of wetting transitions is carefully examined. It is found that the order of wetting transitions is the consequence of the competition between the attractive interaction range and the associating strength of unlike pair molecules. The most intriguing behavior is that it is possible to observe the sequence of wetting transitions along with increasing temperature at two different orders for air–liquid–liquid coexistence at a high pressure. That is, the upper wetting transition is first order and the lower wetting transition is second order. The pressure effect on the order of wetting transitions for liquid–liquid coexistence is also discussed. © *2003 American Institute of Physics.* [DOI: 10.1063/1.1565327]

I. INTRODUCTION

Consider a system of three phases α, β, and γ in equilibrium under Earth's gravitational field. The densities of these three phases are in the order $\rho_\alpha > \rho_\beta > \rho_\gamma$. The α phase can either partially wet or completely wet the interface between two other phases β and γ, as shown in Fig. 1. For the partial-wetting α phase, the α phase forms a droplet suspending at the $\beta-\gamma$ interface with a finite contact angle, as shown in Fig. 1(b). On the other hand, the α phase may spread across the interface to form an intruding film separating the other two phases, known as the complete-wetting α phase. The thickness of the wetting film remains finite due to gravity and depends on the thickness of the β phase. For certain systems the α phase can exhibit both partial wetting and complete wetting at the $\beta-\gamma$ interface under different thermodynamic conditions. The transition of the α phase from a partial-wetting regime to a complete-wetting regime, or vice versa, is called a wetting transition. This remarkable interfacial phenomenon has been the subject of intensive research both theoretically and experimentally in the last three decades due to its importance in many industrial applications.[1]

The wetting transition has been experimentally observed at vapor–liquid,[2–6] liquid–liquid,[7–10] and vapor–solid interfaces.[11–13] Most of the experimental works can be classified into two groups based on their experimental temperature ranges: (1) vapor–liquid–substrate systems such as liquid helium on cesium substrates at extremely low temperatures[11,12] and (2) more conventional binary (or ternary) liquid mixtures at or near room temperature.[2–10] We would like to refer an excellent review article covering all details of the experimental works on wetting transitions.[14]

In fact, there are a tremendous number of binary mixtures accessible to experiments. However, only a small subset of possible binary mixtures has been experimentally observed to study their interfacial wetting behavior. More precisely, most of the experimental studies of binary mixtures in the literature[2–6] belong to the type-II or type-III mixtures of van Konynenburg and Scott.[15] Similarly, the theoretical studies[16,17] have explored the interfacial wetting behaviors for only a limited number of binary mixtures, also restricted to type-II and type-III mixtures only. Recently, the interfacial behavior for associating binary mixtures against a hard wall has been carefully examined by a density functional theory.[18,19] In addition, reentrant wetting and dewetting behaviors have been found in a binary mixture with one self-associating component at vapor–liquid interfaces.[20] However, there is no study, to the best of our knowledge, of the wetting behavior for binary associating mixtures (type VI) at vapor–liquid interfaces in the literature.

According to the classification scheme of van Konynenburg and Scott,[15] a type-VI mixture exhibits two types of closed-loop phase behavior: one at low pressures and the other one at high pressures. At low pressures, a type-VI mix-

a)Author to whom correspondence should be addressed. Electronic mail: ljchen@ccms.ntu.edu.tw

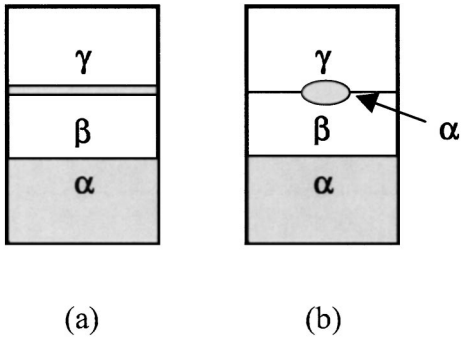

FIG. 1. Wetting behavior of the α phase at the β–γ interface: (a) complete-wetting behavior and (b) partial-wetting behavior.

ture exhibits a three-phase vapor–liquid–liquid coexistence. The three-phase line, known as the triple line, in the phase diagram of pressure–temperature projection is bounded by an upper and a lower critical end point (UCEP and LCEP), where the two liquid phases merge into a single phase. At a fixed high pressure, the type-VI mixtures exhibit two-phase liquid–liquid coexistence.[21] The liquid–liquid immiscibility gap is bounded by an upper and a lower critical solution temperature (UCST and LCST).

In this study, we would like to start with a type-II mixture and this mixture would have a transition to a type-VI mixture by increasing the strength of the associating interaction between unlike pair molecules. Both the phase and wetting behaviors are explored in this associating binary (type-VI) mixture.

This paper is organized as follows: The free energy functional and the details of the calculation procedure are given in the next section. The results for the phase diagrams and wetting behaviors of binary associating (type-VI) mixtures are presented in Sec. III. Finally, in Sec. IV, we conclude our work along with a comparison of the theoretical prediction with experiments.

II. MODEL AND METHODOLOGY

The associating system is modeled as a mixture of equal-sized hard-sphere particles A and B. Each molecule is assumed to have an active site that allows association only between unlike pair molecules to mimic hydrogen bonding.

A. Bulk Helmholtz free energy density

The bulk free energy of the statistical associating fluid theory (SAFT) of Wertheim is composed of the contributions of repulsive, attractive and associating parts. The total Helmholtz free energy density of the mixture f can be written as[22]

$$f = f_R + f_M + f_A, \tag{1}$$

where f_R is the free energy density of the hard-sphere reference fluid, f_M is the van der Waals mean-field term due to the isotropic long-range attraction forces, and f_A is the contribution of the association between unlike pair molecules.

For equal-sized hard-sphere mixtures with a diameter d, the repulsive Helmholtz free energy density is described by the Carnahan–Starling expression[23(a)]

$$f_R = kT \sum_i \rho_i \left[\ln \rho_i - 1 + \frac{4\eta - 3\eta^2}{(1-\eta)^2} \right] \quad (i = \mathrm{A,B}), \tag{2}$$

where k is Boltzmann's constant, T is the temperature, ρ_i is the number density of compound i, and the packing fraction $\eta = (\pi d^3/6)\Sigma_i \rho_i$.

The contribution due to the long-range dispersion forces is treated at the mean-field level[21]

$$f_M = -\tfrac{1}{2} \sum_i \alpha_{ij} \rho_i \rho_j, \tag{3}$$

where the total strength α_{ij} is defined by

$$\alpha_{ij} = -\int d\mathbf{r}\, \phi_{ij}(r) \quad (i,j = \mathrm{A,B}). \tag{4}$$

An isotropic interaction potential of inverse sixth power law decay is applied,[17(e)]

$$\phi_{ij}(r) = -4\varepsilon_{ij} \left(\frac{d}{r + \nu_{ij} d} \right)^6 H(r-d), \tag{5}$$

where ε_{ij} is the energy parameter and H is the Heaviside step function. The parameter ν_{ij} is introduced to adjust the range of attractive interaction between molecules i and j. In our calculation, the total strength α_{ij} is fixed, and thus the phase diagram, coexisting densities, and the critical end points are the same for various ν_{ij}. Figure 2 shows the variation of the interaction potential at three different ν_{ij}'s. Under the condition of constant total strength α_{ij}, the energy parameter ε_{ij} varies accordingly to the parameter ν_{ij}. It is interesting to note that a positive ν_{ij} makes a weaker attractive interaction at short distances and a stronger attractive interaction at long distances, as illustrated in Fig. 2(b). On the other hand, a negative ν_{ij} makes a stronger attractive interaction at short distances and a weaker attractive interaction at long distances.

The association contribution of the free energy is evaluated directly from Wertheim's first-order thermodynamic perturbation theory. For each molecule with only one attractive bonding site, the free energy contribution can be written as[22]

$$f_A = kT \sum_i \rho_i \left[\ln \chi_i - \frac{\chi_i}{2} + \frac{1}{2} \right] \quad (i,j = \mathrm{A,B}), \tag{6}$$

where χ_i is the fraction of non-bonded molecules of type i. The latter quantities are obtained by solving the following mass action equations simultaneously:

$$\chi_\mathrm{A} = \frac{1}{1 + \rho_\mathrm{B} \Delta_\mathrm{AB} \chi_\mathrm{B}}, \tag{7a}$$

$$\chi_\mathrm{B} = \frac{1}{1 + \rho_\mathrm{A} \Delta_\mathrm{AB} \chi_\mathrm{A}}. \tag{7b}$$

The quantity Δ_AB is related to the strength of association between molecules A and B and is approximated[24] by $\Delta_\mathrm{AB} = 4\pi g^\mathrm{HS}(d) K_\mathrm{AB} [\exp(\varepsilon_W/kT) - 1]$. The symbol K_AB is the volume available for association, and ε_W is the energy parameter of association. In addition, $g^\mathrm{HS}(d)$ stands for the contact value of the radial distribution function of the hard-sphere fluid and is given by $g^\mathrm{HS}(d) = (1 - 0.5\eta)/(1-\eta)^3$.[23]

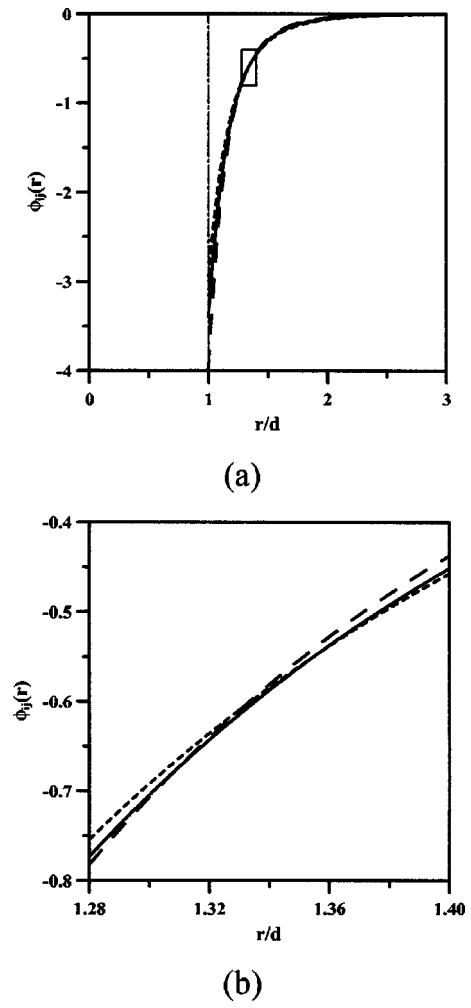

FIG. 2. Variation of the interaction potential ϕ_{ij} at three different ν_{ij}'s: -0.1 ($\varepsilon_{ij}^{*}=0.53$, long-dashed line), 0.0 ($\varepsilon_{ij}^{*}=0.85$, solid line), and 0.1 ($\varepsilon_{ij}^{*}=1.30$, dashed line). Plot (b) is the enlargement of the square area in plot (a) over the regime that the three curves intersect.

B. Phase diagram calculation

At a fixed temperature, the criteria for a multiphase equilibrium require that the pressure and chemical potential of each component should be the same in all phases. Hence the equations used to determine the bulk densities of the N-phase equilibrium system are given as follows:

$$\mu_i(\rho_{\mathrm{A}}^{\mathrm{I}},\rho_{\mathrm{B}}^{\mathrm{I}},T)=\mu_i(\rho_{\mathrm{A}}^{\mathrm{II}},\rho_{\mathrm{B}}^{\mathrm{II}},T)=\cdots=\mu_i(\rho_{\mathrm{A}}^{N},\rho_{\mathrm{B}}^{N},T)$$
$$(i=\mathrm{A},\mathrm{B}), \tag{8}$$

$$P(\rho_{\mathrm{A}}^{\mathrm{I}},\rho_{\mathrm{B}}^{\mathrm{I}},T)=P(\rho_{\mathrm{A}}^{\mathrm{II}},\rho_{\mathrm{B}}^{\mathrm{II}},T)=\cdots=P(\rho_{\mathrm{A}}^{N},\rho_{\mathrm{B}}^{N},T). \tag{9}$$

The chemical potential of species i is given by

$$\mu_i=\left(\frac{\partial f}{\partial \rho_i}\right)_{T,V,\rho_{j\neq i}}, \tag{10}$$

and the equilibrium pressure is thus obtained by

$$P=\sum_i \mu_i\rho_i-f. \tag{11}$$

C. Interfacial properties and density functional theory

The properties of vapor–liquid and liquid–liquid interfaces between coexisting phases of binary associating mixtures can be calculated with the application of density functional theory.[25] The Helmholtz free energy density of a nonuniform binary mixture can be expressed as a functional of the local densities $\rho_i(\mathbf{r})$:

$$F(\rho_i(\mathbf{r}))=\int_V d\mathbf{r}\, f_R(\rho_i(\mathbf{r}))+\int_V d\mathbf{r}\, f_A(\rho_i(\mathbf{r}))$$
$$+\tfrac{1}{2}\sum_{ij}\int\int_V d\mathbf{r}\, d\mathbf{r}'$$
$$\times\phi_{ij}(|\mathbf{r}-\mathbf{r}'|)\rho_i(\mathbf{r})\rho_j(\mathbf{r}'), \tag{12}$$

where $f_R(\rho_i(\mathbf{r}))$ and $f_A(\rho_i(\mathbf{r}))$ are considered to be functions of local densities $\rho_i(\mathbf{r})$ and are given by Eqs. (2) and (6).

Consider a planar interface between coexisting phases, the grand potential functional $\Omega(\rho_i(\mathbf{r}))$ for an inhomogeneous binary mixture can be written as follows:

$$\Omega(\rho_i(\mathbf{r}))=F(\rho_i(\mathbf{r}))-\sum_i \mu_i\int_V d\mathbf{r}\,\rho_i(\mathbf{r}), \tag{13}$$

where V is the volume of the system. The equilibrium density profiles across an interface are obtained through the minimization of the $\Omega(\rho_i(\mathbf{r}))$.[25] Setting the derivative of $\Omega(\rho_i(\mathbf{r}))$ with respect to $\rho_i(\mathbf{r})$ equal to zero yields a set of integral equations at equilibrium chemical potentials μ_i:

$$\mu_R(\rho_i(\mathbf{r}))+\mu_A(\rho_i(\mathbf{r}))$$
$$=\mu_i-\sum_{ij}\int_V d\mathbf{r}'\,\phi_{ij}(|\mathbf{r}-\mathbf{r}'|)\rho_j(\mathbf{r}') \quad (i=A,B), \tag{14}$$

where $\mu_R(\rho_i(\mathbf{r}))=\partial f_R(\rho_i(\mathbf{r}))/\partial\rho_i(\mathbf{r})$ and $\mu_A(\rho_i(\mathbf{r}))=\partial f_A(\rho_i(\mathbf{r}))/\partial\rho_i(\mathbf{r})$.

The last equation can be numerically solved by an iterative method.[17(e)] The equilibrium bulk densities, which are evaluated via the standard method mentioned in the previous section, provide the boundary conditions for the Euler–Lagrange equations, Eq. (14). Once the equilibrium density profiles across an interface are determined, the interfacial tension σ is easily evaluated from

$$\sigma=\frac{\Omega(\rho_i(r))+PV}{A}, \tag{15}$$

where A represents the planar interfacial area between coexisting phases. Once the interfacial tensions are obtained, the wetting behavior can be determined by examining the interfacial tensions obey Antonow's rule[26] or Neumann's inequality.[27]

D. Wetting transition temperature and order of wetting transitions

Consider the system of three phases α, β, and γ at equilibrium. There are three interfacial tensions $\sigma_{\alpha\beta}$, $\sigma_{\alpha\gamma}$, and $\sigma_{\beta\gamma}$, which are the surface tensions of the α–β, α–γ, and β–γ interfaces, respectively, in the three-phase coexisting system. According to the wetting behavior of the α phase at

the $\beta-\gamma$ interface, the relationship of three interfacial tensions can be classified into two cases: (i) complete-wetting α phase, the interfacial tensions satisfy Antonow's rule,[26] $\sigma_{\beta\gamma}=\sigma_{\alpha\beta}+\sigma_{\alpha\gamma}$, as shown in Fig. 1(a) and (ii) partial-wetting α phase, the interfacial tensions obey Neumann's inequality,[27] $\sigma_{\beta\gamma}<\sigma_{\alpha\beta}+\sigma_{\alpha\gamma}$, as shown in Fig. 1(b). The wetting transition temperature T_W is defined as the temperature at which the relation of interfacial tensions alters from Neumann's inequality to Antonow's rule or vice versa. In this study, we first determine three interfacial tensions as a function of temperature and then evaluate the temperature dependence of interfacial tension difference $\Delta\sigma(T)=\sigma_{\alpha\beta}(T)+\sigma_{\alpha\gamma}(T)-\sigma_{\beta\gamma}(T)$. When the interfacial tension difference $\Delta\sigma$ vanishes at T_W, a wetting transition from partial wetting to complete wetting occurs.

In this study, we also determine the order of wetting transitions by the method of Tarazona and Evans.[17(d)] A wetting transition is said to be first order if the temperature dependence of wetting film thickness shows a discontinuity at T_W. On the other hand, if the film thickness grows gradually and diverges at T_W, the wetting transition is identified as second order.[6]

III. RESULTS AND DISCUSSION

In this section, the wetting behaviors of type-VI mixtures are examined both at low pressures, $P^*<0.07$, and at high pressures, $P^*\geqslant 1.0$. All the calculations are performed in reduced units: $T^*=kT/\varepsilon_{AA}$, $\mu_i^*=\mu_i/\varepsilon_{AA}$, $P^*=Pd^3/\varepsilon_{AA}$, $\varepsilon_{ij}^*=\varepsilon_{ij}/\varepsilon_{AA}$, $\varepsilon_W^*=\varepsilon_W/\varepsilon_{AA}$, $\alpha_{ij}^*=3\alpha_{ij}/16\pi d^3\varepsilon_{AA}$, $K_{AB}^*=K_{AB}/d^3$, and $\rho_i^*=\rho_i d^3$. Note that $K_{AB}^*=10^{-5}$ and $\nu_{AA}=\nu_{BB}=0$ in all our calculations.

A. Low-pressure regime: Vapor–liquid–liquid coexistence

For comparison, we first present the results of nonassociating, $\varepsilon_W^*=0$, and equal-ranged, $\nu_{AB}=0.0$ $(=\nu_{AA}=\nu_{BB})$ mixtures. The energy parameters $\alpha_{AA}^*=1.0$, $\alpha_{BB}^*=1.2$, and $\alpha_{AB}^*=0.85$ are chosen for the model binary mixture. This mixture exhibits a liquid–liquid miscibility gap with an UCEP where the two liquid phases α (A rich) and β (B rich) merge into a single liquid phase coexisting with its vapor phase γ. The phase behavior of the three-phase coexisting regime is shown in Fig. 3(a). This mixture is classified as the type-II mixture of van Konynenburg and Scott.[15]

Consider the wetting behavior of the α phase at the $\beta-\gamma$ interface for the system under three-phase coexistence. A wetting transition occurs at $T_W=1.148$, while the system is approaching its UCEP ($T_{UCEP}=1.280$) from below. When $T^*\geqslant T_W$, the α phase wets the $\beta-\gamma$ interface. In other words, a small amount of the α phase forms an intruding layer separating β and γ phases, as illustrated in Fig. 1(a). Besides, this wetting transition is found to be second order. These results are consistent with a previous study of type-II mixtures by Tarazona *et al.*[17(e)]

Now, turn on the effect of associating interaction between unlike pair molecules by increasing the strength of ε_W^*. For small ε_W^*—say, $\varepsilon_W^*<5$—the temperature–composition projection along its triple line is quite insensitive to association at all temperatures. When ε_W^* is gradually increased to higher strengths—say, $\varepsilon_W^*\geqslant 6$—the association effect is enhanced, especially at low temperatures. The association effect can be easily delineated by the number density of bonded molecules ρ_{bond}^*, which is defined as $\rho_{bond}^*=\rho_A^*(1-\chi_A)=\rho_B^*(1-\chi_B)$. It is interesting to note that ρ_{bond}^*

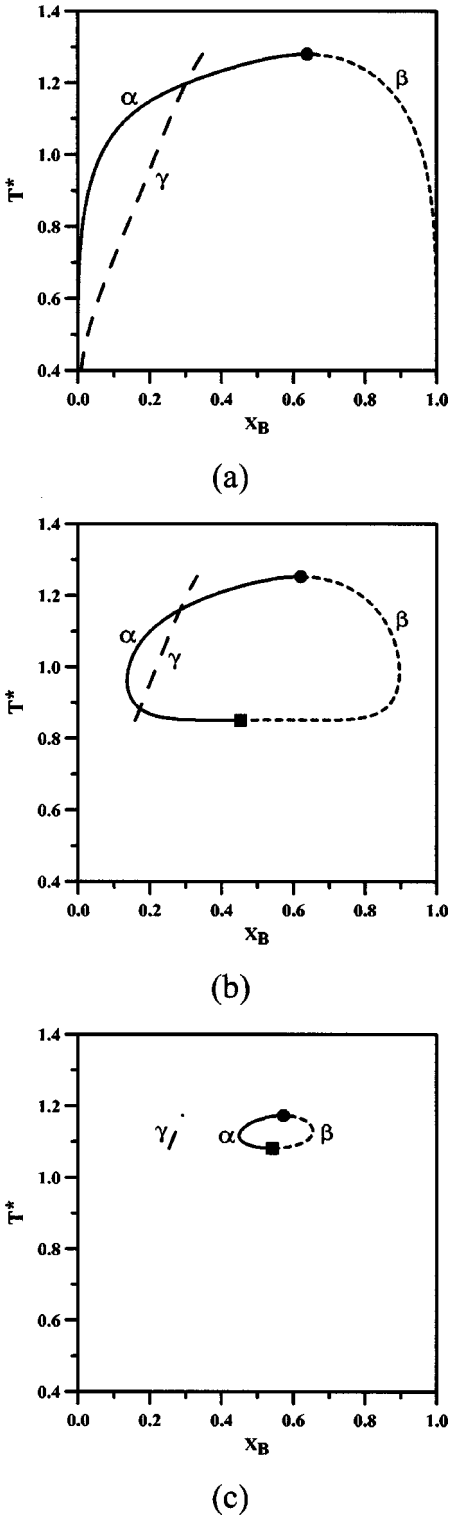

FIG. 3. Vapor–liquid–liquid equilibrium of the binary mixture with $\alpha_{AA}^*=1.0$, $\alpha_{BB}^*=1.2$, and $\alpha_{AB}^*=0.85$ and (a) $\varepsilon_W^*=0.0$, (b) $\varepsilon_W^*=7.85$, and (c) $\varepsilon_W^*=9.0$. The symbol α stands for the A-rich liquid phase (solid curves), β for the B-rich liquid phase (dotted curves), and γ for the vapor phase (long dashed curves). ●: UCEP. ■: LCEP.

in the α phase almost coincides with ρ^*_{bond} in the β phase, while ρ^*_{bond} in the γ phase is too small ($<10^{-5}$) to be perceptible. When $\varepsilon^*_W<5$, over the entire three-phase coexisting regime the quantity ρ^*_{bond} remains consistently small. Therefore, the phase behavior remains insensitive to ε^*_W for $\varepsilon^*_W<5$. On the other hand, for large ε^*_W—say, $\varepsilon^*_W\geqslant 6$—$\rho^*_{\text{bond}}$ monotonically increases as the temperature decreases. Especially at low temperatures, ρ^*_{bond} increases dramatically. This phenomenon is consistent with the temperature dependence of hydrogen-bonding formation. It is easier to form a hydrogen bond at low temperatures. When the temperature is increased, many hydrogen bonds are broken due to larger thermal fluctuations that make the number of hydrogen bonds decrease.

With further increase in ε^*_W, the miscibility of compounds A and B becomes better at low temperatures due to the association effect. Eventually, when $\varepsilon^*_W=7.85$, a LCEP emerges to form a closed loop, where the two liquid phases α and β become identical and coexist with its vapor phase γ, as shown in Fig. 3(b). This association effect induces a transition of phase behavior of the system from type-II to type-VI mixture, as shown in Fig. 3. That is, when $\varepsilon^*_W<7.85$, the system belongs to type-II mixtures; when $\varepsilon^*_W\geqslant 7.85$ the system falls into the category of type-VI mixtures, as shown in Fig. 4. The closed loop would shrink with further enhancement of association interaction, as shown in Fig. 3(c). Finally, the closed loop would disappear for $\varepsilon^*_W>9.03$.

In the meantime, as the phase behavior of the binary mixture evolves from type II to type VI, another wetting transition temperature emerges accompanying the occurrence of the LCEP. Consider the system with relatively strong association $\varepsilon^*_W=8.0$. While the system temperature approaches either its UCEP from below or its LCEP from above, a wetting transition from a partial-wetting to a complete-wetting α phase occurs. Correspondingly, an upper wetting transition temperature $T_{\text{UW}}=1.040$ and a lower wetting transition temperature $T_{\text{LW}}=0.985$ are found. When $T_{\text{UW}}>T^*>T_{\text{LW}}$, the α phase exhibits partial wetting. Beyond these two wetting transition temperatures, the α phase completely wets the β–γ interface. In other words, the wetting behavior of the α phase at the β–γ interface would go through a sequence of complete wetting→partial wetting→complete wetting along with increasing temperature as schematically shown in Fig. 5. This sequential wetting transition is the so-called reentrant wetting.[20]

Figure 4 illustrates the variation of the critical end points and the wetting transition temperatures as a function of ε^*_W. For type-II mixtures, both T_{UW} and T_{UCEP} remain almost constant for $\varepsilon^*_W<5$, as one can see in Fig. 4(a). For type-VI mixtures ($\varepsilon^*_W\geqslant 7.85$), both T_{UW} and T_{LW} are driven further away from their corresponding critical end points with increasing ε^*_W. Consequently, the regime of the partial-wetting α phase shrinks when ε^*_W increases. Eventually, T_{UW} and T_{LW} merge before the closed-loop phase behavior disappears. For very strong associating cases $\varepsilon^*_W>8.05$, the α phase wets the β–γ interface over the entire three-phase coexistence regime, as shown in Fig. 4(b).

The attractive range parameter ν_{AB} has a strong effect on both T_{W} and the order of a wetting transition. For a nonassociating mixture ($\varepsilon^*_W=0$) with $\nu_{\text{AB}}>0$, the wetting transition is first order as the range of the A–B attractive potential is longer than that of the A–A and B–B potentials.[17(e)] Figure 6 illustrates the effect of ν_{AB} on T_{W} and the order of wetting

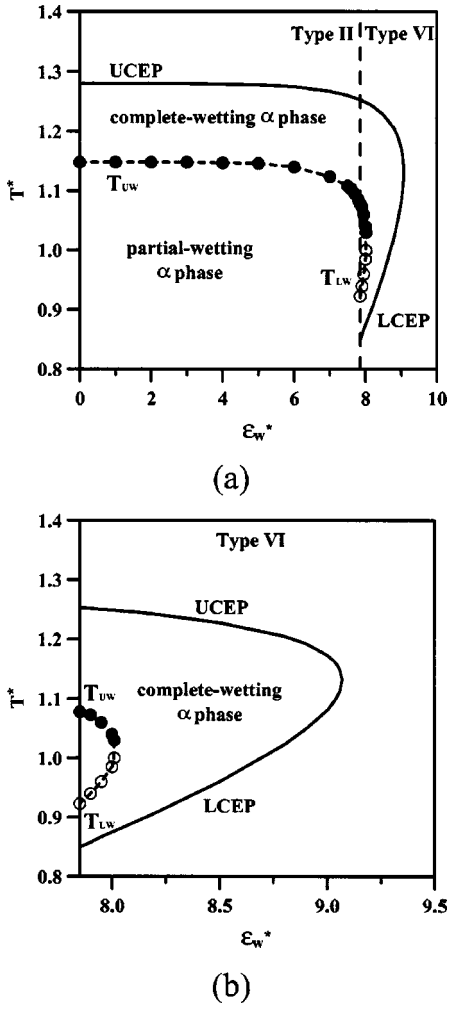

FIG. 4. Effect of ε^*_W on critical end points and wetting transition temperatures with a transition from type-II to type-VI mixtures. Plot (b) is the enlargement of plot (a) over the regime of type-VI mixtures.

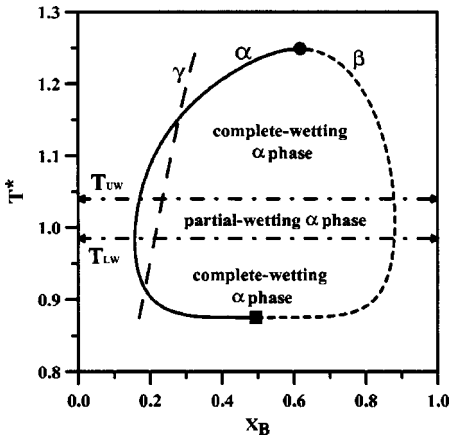

FIG. 5. Temperature–composition projection and the wetting behavior of α phase at the β–γ interface for the binary mixture with $\alpha^*_{\text{AA}}=1.0$, $\alpha^*_{\text{BB}}=1.2$, $\alpha^*_{\text{AB}}=0.85$, and $\varepsilon^*_W=8.0$. ●: UCEP. ■: LCEP.

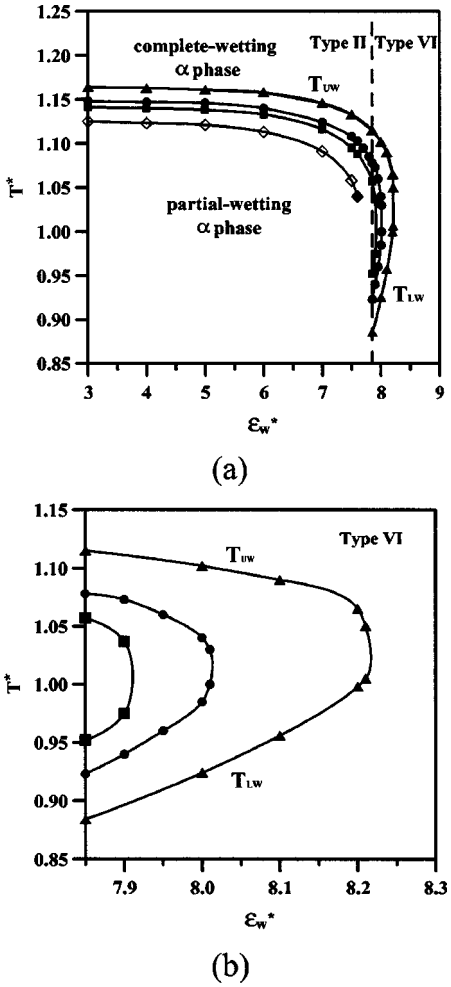

FIG. 6. Variation of wetting transition temperatures at different ν_{AB}'s: -0.03 (▲), 0.00 (●), 0.01 (■), and 0.03 (◇, ◆). Plot (b) is the enlargement of plot (a) over the regime of type-VI mixtures. The solid symbol represents a second-order wetting transition, and and the open symbol for a first-order wetting transition.

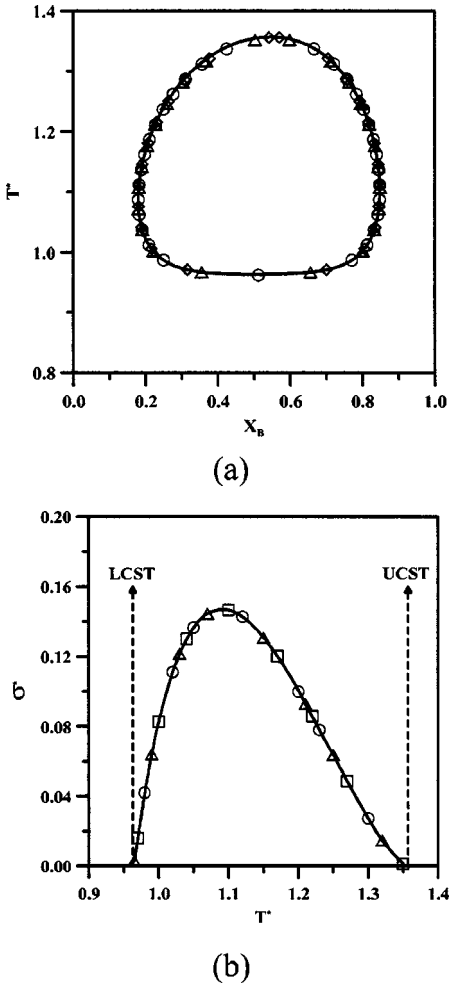

FIG. 7. (a) Phase diagram and (b) interfacial tensions. Liquid–liquid coexistence at a fixed pressure $P^*=1.0$. The solid curves represent the results calculated from the binary A+B mixture. The results for pseudobinary A+B+C mixtures are given at three different α_{CC}^*'s: 0.15 (○), 0.25 (□), and 0.35 (△).

transitions along with increasing ε_W^*. For $\nu_{AB}=0.01$, the regime of the partial-wetting α phase slightly shrinks and the order of wetting transitions is found to be on the borderline between the first and second orders. For a larger ν_{AB}—say, $\nu_{AB}=0.03$—T_W decreases dramatically and the wetting transition switches to first order for small ε_W^*, but tends to be second order for $\varepsilon_W^*>7.5$. If ε_W^* is further increased, $\varepsilon_W^*>7.7$, the system exhibits the complete-wetting α phase over the entire triple line. For a negative ν_{AB}—say, $\nu_{AB}=-0.03$—the regime of the partial-wetting α phase is broadened while the order of wetting transitions always remains second order. It could be reminisced that a positive value of ν_{AB} extends the range of attractive interaction between molecules A and B and switches the order of wetting transitions from second to first order while a negative ν_{AB} prefers the transitions to be second order. On the other hand, a sufficient large ε_W^*, which introduces a strong short-ranged interaction between A and B, would demolish the effect of ν_{AB} and change the order of wetting transitions from first to second order. Conclusively, a positive ν_{AB} favors a first-order wetting transition while a large ε_W^* favors a second-order wetting transition. The order of a wetting transition can be considered as the outcome of the competition between ν_{AB} and ε_W^*.

Figure 6(b) shows the variation of wetting transition temperatures at three different ν_{AB}'s as a function of ε_W^*. It should be noted that all the wetting transitions along the triple line in Fig. 6(b) are second order.

B. High-pressure regime: Liquid–liquid coexistence

Following the previous section, the parameters of a binary mixture, $\alpha_{AA}^*=1.0$, $\alpha_{BB}^*=1.2$, $\alpha_{AB}^*=0.85$, and $\varepsilon_W^*=8.1$, are applied to mimic a type-VI mixture at high pressures. Figure 7(a) shows the result of phase behavior at $P^*=1.0$. That is a typical immiscibility gap of type-VI mixtures, a closed-loop behavior. The mole fraction of molecules B, x_B, in Fig. 7(a) is defined as $x_B=\rho_B^*/(\rho_A^*+\rho_B^*)$. It should be noted that the temperature range of immiscibility (ΔT = UCST−LCST) increases with increasing pressure. On the other hand, the interfacial tension between A-rich (α) and B-rich (β) phases can be evaluated by following the method described in Sec. II, and the results are given in Fig. 7(b).

It should be noted that wetting behavior always involves three phases. Now, we have the system of two immiscible liquids. ''Air'' is chosen to be the third phase. That is, we would like to examine the wetting behavior of the two immiscible liquids against air. However, there is no way for us to use the density functional theory to calculate the surface tension of any liquid (α or β) phase against air. It is essential to have equilibrium compositions of two coexisting phases to calculate the interfacial tension of the interface between two coexisting phases by the density functional theory. For the time being, we only have two-liquid phase coexisting. There is no coexisting ''air'' phase. Certainly, no equilibrium compositions of air phase can be applied to Eqs. (13) and (15) of the density functional theory. Therefore, a third component C is introduced to the system to mimic the ''air'' phase. The component C should be inert and have negligible effects on the phase and interfacial behavior of original A+B mixtures.

To ensure the component C mimicking inert air, both the parameters α^*_{AC} and α^*_{BC} are set to zero and a relatively small energy parameter between C molecules, α^*_{CC}, is adopted. Equations (8) and (9) are applied to determine the equilibrium compositions of three-phase coexisting (two liquids and air) for ternary (A+B+C) mixtures. Figure 7(a) shows the effect of introducing the component C on the phase behavior (immiscibility gap) at three different α^*_{CC}'s: 0.15 (○), 0.25 (□), and 0.35 (△). It is obvious that the introduction of the component C has ''almost'' no effect on the closed-loop behavior of binary (A+B) mixtures. In fact, the solubility of the component C in each liquid phase (α or β) is very small. More precisely, the mole fraction of the component C in the liquid (α or β) phase is always less than 0.0001. Apply the equilibrium compositions of three-phase coexisting for ternary (A+B+C) mixtures to the density functional theory to calculate the interfacial tension between α and β phase. The results of the interfacial tensions at three different α^*_{CC}'s: 0.15 (○), 0.25 (□), and 0.35 (△) are also given in Fig. 7(b). As expected, the introduction of the component C also has no effect on the interfacial tension of binary (A+B) mixtures. In summary, both phase diagrams and interfacial tensions remain unchanged when the component C is introduced to the mixture A+B as an inert phase. With an additional air phase, the surface tensions of both liquid phases against air can be thus determined. Consequently, wetting behavior of the three-phase coexisting (two liquids and air) system can be explored. In the following, $\alpha^*_{CC}=0.15$ is applied for further discussion on wetting behavior of the α phase on the surface of the β phase against air (defined as the γ phase hereafter).

It is found that the wetting behavior of the α phase of the pseudobinary mixtures at a fixed high pressure is strikingly similar to that along the triple line at low pressures, described in the previous section. There are two critical temperatures, UCST and LCST, for the closed-loop phase behavior at $P^*=1.0$. When the temperature T is in the middle of two critical temperatures, the α phase exhibits a partial-wetting behavior. While the temperature is driven close to either its UCST (=1.370) or its LCST (=0.894), a wetting transition from partial wetting to complete wetting occurs. The corresponding upper and lower wetting transition temperatures are $T_{UW}=1.255$ and $T_{LW}=0.934$. That is, the α phase wets the β–γ interface when the system temperature T falls into following two regimes: $T_{UW}<T^*<$UCST and LCST$<T^*<T_{LW}$, as schematically shown in Fig. 1(a). Again, the complete-wetting phase is mainly composed of the liquid with a smaller energy parameter: namely, the A-rich (α) phase.

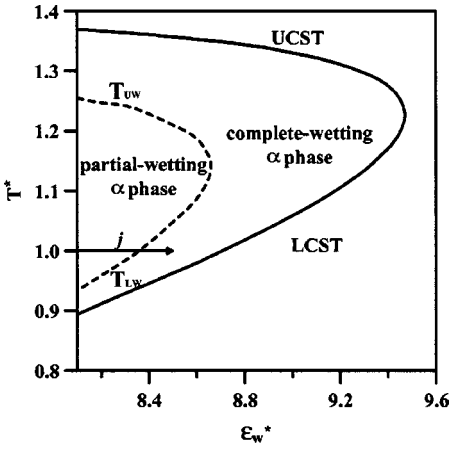

FIG. 8. Effect of ε^*_W on the critical solution and wetting transition temperatures at $P^*=1.0$.

Figure 8 shows the effect of ε^*_W on the critical solution temperatures and the wetting transition temperatures. For very strong associating mixtures $\varepsilon^*_W>8.7$, the α phase wets the β–γ interface over the entire liquid–liquid coexisting region. The wetting transition occurs only when $\varepsilon^*_W<8.7$. Along a constant temperature—say, $T^*=1.0$ in Fig. 8—the increase in ε^*_W would drive wetting behavior of the α phase from partial wetting to complete wetting.

All the wetting transitions in Fig. 8 are always second order, since $\nu_{AB}=0$. As mentioned above, the order of the wetting transition can be considered as the outcome of the competition between ν_{AB} and ε^*_W. Therefore, we would like to further explore the effect of ν_{AB} on the wetting transition temperature and the order of wetting transitions for strong association mixtures $\varepsilon^*_W=8.1$. Figure 9(a) shows the variations of T_W and the order of wetting transitions as a function of ν_{AB} at $P^*=1.0$. In analog to the phenomena observed along the triple line, the increase in ν_{AB} would narrow down the temperature window of the partial-wetting α phase and switch the wetting transition from second to first order. When ν_{AB} is further increased beyond 0.052, the α phase wets the β–γ interface over the entire liquid–liquid coexisting region. Both the upper and lower wetting transitions for small ν_{AB} (<0.01) are second order, as shown in Fig. 9(a). When ν_{AB} is further increased up to 0.03, both the upper and lower wetting transitions become first order, as expected.

The most intriguing phenomenon is that when $\nu_{AB}=0.02$, the upper wetting transition already becomes first order and the lower wetting transition still remains second order, as shown in Fig. 9(a). That is, for the mixture of $\nu_{AB}=0.02$, a first-order wetting transition is observed when the system temperature is approaching its UCST. It is well understood that the association interaction has a stronger contribution at low temperatures, which would favor a second

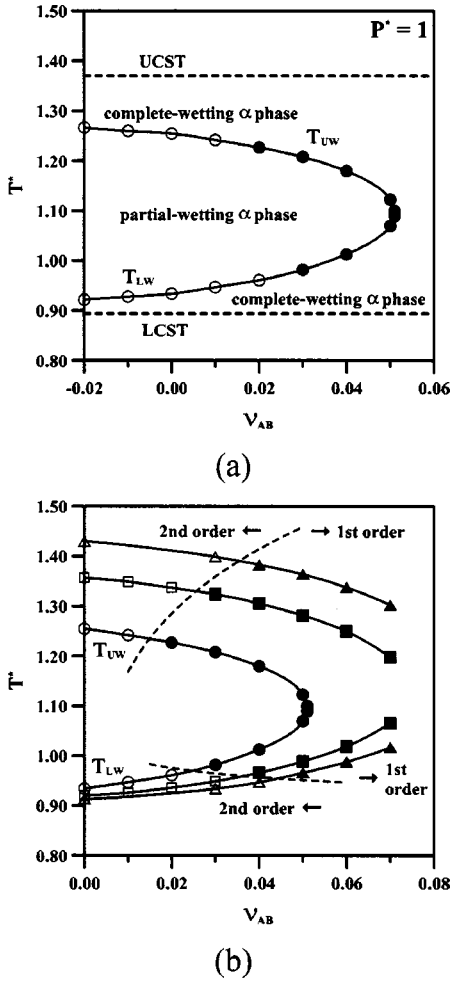

FIG. 9. (a) Variation of wetting transition temperatures as a function of ν_{AB} at $P^*=1.0$. (b) The pressure effect on the wetting transition temperatures: $P^*=1.0$ (●, ○), $P^*=2.0$ (□, ■), and $P^*=3.0$ (△, ▲). The open symbols representing the wetting transitions are second order and the filled symbols for first order.

order. Thus, when the system temperature is approaching its LCST, one would observe a second-order wetting transition. This prediction provides the possibility of the existence of having both first- and second-order wetting transitions in a type-VI mixture of a closed-loop phase behavior.

Figure 9(b) shows the pressure effect upon the wetting behavior as well as the order of wetting transitions. As mentioned above, the temperature range of immiscibility increases with increasing pressure. It is interesting to note that the temperature range of the partial-wetting α phase ($\Delta T = T_{UW} - T_{LW}$) also increases with increasing pressure. The borderlines separating first- and second-order wetting transitions are sketched in Fig. 9(b). When the system pressure is raised, the borderlines shift to a higher value of ν_{AB}. It is well understood that the increase in pressure would shorten the distance between molecules to enhance the short-ranged contribution. The associating effect is thus strengthened along with increasing pressure. As a consequence, a second-order wetting transition is favored even at a higher pressure under the condition of a fixed ν_{AB}.

IV. CONCLUSION

In this study, the SAFT of Wertheim is applied to successfully describe the type-VI mixture of the classification scheme of van Konynenburg and Scott. For type-VI mixtures closed-loop phase diagrams are obtained both at low pressures (along its triple line, $P^*<0.07$) and at a fixed high pressure ($P^*\geqslant 1.0$). For the regime of low pressures, type-VI mixtures exhibit three-phase vapor–liquid–liquid coexistence and have two critical end points UCEP and LCEP, where two liquid phases merge into a single liquid phase coexisting with its vapor phase. With increasing the temperature a sequence of wetting transitions, complete wetting→partial wetting→complete wetting, of the denser liquid α phase at the surface of the other liquid β phase against its vapor γ phase is observed.

For the regime of high pressures, type-VI mixtures exhibit two-phase liquid–liquid coexistence at a fixed pressure and also have two critical points UCST and LCST, where two liquid phases merge into a single liquid phase. Since wetting behavior always involves three phases, a third inert air phase is introduced. Under the condition of a fixed pressure, when the temperature is increased again a sequence of wetting transitions, complete wetting→partial wetting →complete wetting, of the denser liquid α phase at the surface of the other liquid β phase against air is observed.

It is also demonstrated that the order of wetting transitions can be resolved by the competition between the attractive interaction range and the associating effect between unlike molecule pairs. A stronger attractive interaction at long distances facilitates a first-order wetting transition while a strong associating interaction in favor of a second-order transition. The most intriguing phenomenon is that it is possible to observe for certain systems of air–liquid–liquid coexistence at a fixed high pressure the upper and lower wetting transitions are at two different orders. That is, the upper wetting transition is first order and the lower one is second order.

The only experimental exploration of wetting behavior of type-VI mixtures, to the best of our knowledge, at liquid–liquid coexistence was done by Kahlweit and Busse[28] for the binary water+nonionic amphiphile (C_iE_j) mixtures, where C_iE_j is the abbreviation of a nonionic surfactant polyoxyethylene alcohol $C_iH_{2i+1}(OCH_2CH_2)_jOH$. The wetting behaviors of the aqueous C_8E_j homologues ($j=0-3$) mixtures at a constant temperature were investigated. With a stepwise increase of the number of oxyethylene groups j from 0 to 3 at 25 °C, the contact angle of a droplet of the C_8E_j-rich phase at the surface of the aqueous phase evolves from about less than $\pi/2$ to close to 2π, indicating a tendency of the existence of the wetting transition from partial wetting to dewetting. That is equivalent to the wetting transition of the aqueous phase at the surface of the C_8E_j-rich phase from partial wetting to complete wetting. It is well understood that the system with a larger j at a fixed i possesses a higher LCST.[29] Hence the increase in j at a constant temperature could be considered as driving the system closer to its LCST. Consequently, if the number of oxyethylene groups j is further increased, a wetting transition for the aqueous phase at the surface of the C_8E_j-rich phase from partial wetting to complete wetting is expected. That is, a wetting transition from

partial wetting to complete wetting should be observed as the system is brought close to its LCST.

It is found that wetting behavior predicted in this study is comparable to the binary water$+C_iE_j$ mixtures by assigning molecules A and B as water and C_iE_j, respectively. For instance, to start with a partial-wetting α phase at a low temperature, $T^*=1.0$ and $\varepsilon_W^*=8.1$. If ε_W^* is increased isothermally, a transition from a partial-wetting to a complete-wetting α phase occurs near $\varepsilon_W^*=8.4$, as illustrated in Fig. 8. The increase in ε_W^* is equivalent to the increase in the number of oxyethylene groups j. This prediction is consistent with Kahlweit and Busse's observation on the binary water $+C_8E_j$ mixture with varying j at 25 °C. In addition, our model also predicts that there exists a wetting transition of water-rich (α) phase at the surface of the amphiphile-rich (β) phase while the system temperature is driven to approach its LCST from above, also in accordance with Kahlweit and Busse's conjecture[28] based on their experimental evidence.

[1] M. Schick, in *Liquids at Interfaces (Les Houches Session XLVIII, 1988)* edited by J. Charvolin, J. F. Joanny, and J. Zinn-Justin (Elsevier, Amsterdam, 1990), p. 415.
[2] M. R. Moldover and J. W. Cahn, Science **207**, 1073 (1980).
[3] J. W. Schmidt and M. R. Moldover, J. Chem. Phys. **79**, 379 (1983).
[4] M. Kahlweit, G. Busse, D. Haase, and J. Jen, Phys. Rev. A **38**, 1395 (1988).
[5] E. Carrillo, V. Talanquer, and M. Costas, J. Phys. Chem. **100**, 5888 (1996).
[6] (a) D. Bonn, H. Hellay, and G. H. Wegdam, Phys. Rev. Lett. **69**, 1975 (1992); (b) K. Ragil, J. Meunier, D. Broseta, J. O. Indekeu, and D. Bonn, *ibid.* **77**, 1532 (1996); (c) D. Ross, D. Bonn, and J. Meunier, Nature (London) **400**, 737 (1999); (d) E. Bertrand, H. Dobbs, D. Broseta, J. O. Indekeu, D. Bonn, and J. Meunier, Phys. Rev. Lett. **85**, 1282 (2000).
[7] (a) M. Kahlweit, R. Strey, P. Firman, D. Haase, J. Jen, and R. Schomacker, Langmuir **4**, 499 (1988); (b) M. Aratono and M. Kahlweit, J. Chem. Phys. **95**, 8578 (1991).
[8] Y. Seeto, J. E. Puig, L. E. Scriven, and H. T. Davis, J. Colloid Interface Sci. **96**, 360 (1983).
[9] D. H. Smith and G. L. Covatch, J. Chem. Phys. **93**, 6870 (1990).
[10] (a) L.-J. Chen, J.-F. Jeng, M. Robert, and K. P. Shukla, Phys. Rev. A **42**, 4716 (1990); (b) L.-J. Chen and M.-C. Hsu, J. Chem. Phys. **97**, 690 (1992); (c) L.-J. Chen and W.-J. Yan, *ibid.* **98**, 4830 (1993); (d) L.-J. Chen, W.-J. Yan, M.-C. Hsu, and D.-L. Tyan, J. Phys. Chem. **98**, 1910 (1994); (e) L.-J. Chen, M.-C. Hsu, S.-T. Lin, and S.-Y. Yang, *ibid.* **99**, 4687 (1995); (f) L.-J. Chen, S.-Y. Lin, and J.-W. Xyu, J. Chem. Phys. **104**, 225 (1996); (g) M.-C. Yeh and L.-J. Chen, *ibid.* **115**, 8575 (2001).
[11] J. Klier, P. Stefanyi, and A. F. G. Wyatt, Phys. Rev. Lett. **75**, 3709 (1995).
[12] E. Rolley and C. Guthman, J. Low Temp. Phys. **106**, 81 (1997).
[13] J. Y. Wang, S. Betelu, and B. M. Law, Phys. Rev. Lett. **83**, 3677 (1999).
[14] D. Bonn and D. Ross, Rep. Prog. Phys. **64**, 1085 (2001).
[15] P. H. van Konynenburg and R. L. Scott, Philos. Trans. R. Soc. London, Ser. A **298**, 495 (1980).
[16] (a) S. Dietrich and A. Latz, Phys. Rev. B **40**, 9204 (1989); (b) T. Getta and S. Dietrich, Phys. Rev. E **47**, 1856 (1993).
[17] (a) M. M. Telo da Gama and R. Evans, Mol. Phys. **48**, 229 (1983); (b) **48**, 251 (1983); (c) **48**, 687 (1983); (d) P. Tarazona and R. Evans, *ibid.* **48**, 799 (1983); (e) P. Tarazona, M. M. Telo da Gama, and R. Evans, *ibid.* **49**, 283 (1983).
[18] (a) C. J. Segura, W. G. Chapman, and K. P. Shukla, Mol. Phys. **90**, 759 (1997); (b) C. J. Segura, J. Zhang, and W. G. Chapman, *ibid.* **99**, 1 (2001).
[19] A. Patrykiejew and S. Sokolowski, J. Phys. Chem. B **103**, 4466 (1999).
[20] C. Pérez, P. Roquero, and V. Talanquer, J. Chem. Phys. **100**, 5913 (1994).
[21] J. S. Rowlinson and F. L. Swinton, *Liquid and Liquids Mixtures*, 3rd ed. (Butterworth, London, 1982).
[22] G. Jackson, Mol. Phys. **72**, 1365 (1991).
[23] (a) N. F. Carnahan and K. E. Starling, J. Chem. Phys. **51**, 635 (1969); (b) T. Boublík, *ibid.* **53**, 471 (1970).
[24] G. Jackson, W. G. Chapman, and K. E. Gubbins, Mol. Phys. **65**, 1 (1988).
[25] R. Evans, Adv. Phys. **28**, 143 (1979).
[26] F. P. Buff, in *Encyclopedia of Physics*, edited by S. Flugge (Springer, Berlin, 1960), Vol. 10, Sec. 7, pp. 298 and 299.
[27] G. N. Antonow, J. Chem. Phys. **5**, 372 (1907).
[28] M. Kahlweit and G. Busse, J. Chem. Phys. **91**, 1339 (1989).
[29] K. V. Schubert, R. Strey, and M. Kahlweit, J. Colloid Interface Sci. **141**, 21 (1991).